# Supplementary Information

# of

# A parameterization of sulfuric acid-dimethylamine nucleation and its application in three-dimensional modeling

Yuyang Li[1, #], Jiewen Shen[1, 2, #], Bin Zhao[1, 2, *], Runlong Cai[3], Shuxiao Wang[1, 2], Yang Gao[4], Manish Shrivastava[5], Da Gao[1, 2], Jun Zheng[6], Markku Kulmala[2, 7, 8], Jingkun Jiang[1, *]

[1]State Key Joint Laboratory of Environment Simulation and Pollution Control, School of Environment, Tsinghua University, 100084 Beijing, China
[2]State Environmental Protection Key Laboratory of Sources and Control of Air Pollution Complex, Beijing, 100084, China
[3]Institute for Atmospheric and Earth System Research/Physics, Faculty of Science, University of Helsinki, 00014 Helsinki, Finland
[4]Key Laboratory of Marine Environment and Ecology, Ministry of Education, Ocean University of China, Qingdao 266100, China
[5]Brian Gaudet, Pacific Northwest National Laboratory, Richland, Washington, USA
[6]School of Environmental Science and Engineering, Nanjing University of Information Science & Technology, Nanjing 210044, China
[7]Aerosol and Haze Laboratory, Beijing Advanced Innovation Center for Soft Matter Science and Engineering, Beijing University of Chemical Technology, 100029 Beijing, China
[8]Joint International Research Laboratory of Atmospheric and Earth System Sciences, School of Atmospheric Sciences, Nanjing University, Nanjing, China

[#] These authors contributed equally

[*]*Correspondence to*: Bin Zhao (bzhao@mail.tsinghua.edu.cn) and Jingkun Jiang (jiangjk@tsinghua.edu.cn)

## 1 Lookup table for necessary parameters

**Table S1. Lookup table for $G(i,j)$ and $H(i)$ in the parameterization**

| $G(i,j)$ | | $i$ | | | | | | |
|---|---|---|---|---|---|---|---|---|
| | | 1 | 2 | 3 | 4 | 5 | 6 | 7 |
| $j$ | 1 | 0.71 | 0.96 | 0.86 | 0.91 | 1.01 | 1.15 | 1.28 |
| | 2 | 0.96 | 1.20 | 1.20 | 1.31 | 1.47 | 1.70 | 1.90 |
| | 3 | 0.86 | 1.20 | 1.00 | 1.01 | 1.11 | 1.22 | 1.32 |
| | 4 | 0.91 | 1.31 | 1.01 | 0.99 | 1.06 | 1.13 | 1.20 |
| | 5 | 1.01 | 1.47 | 1.11 | 1.06 | 1.12 | 1.18 | 1.24 |
| | 6 | 1.15 | 1.70 | 1.22 | 1.13 | 1.18 | 1.20 | 1.24 |
| | 7 | 1.28 | 1.90 | 1.32 | 1.20 | 1.24 | 1.24 | 1.26 |
| $H(i)$ | | 1.00 | 0.89 | 0.63 | 0.51 | 0.43 | 0.34 | 0.29 |

## 2 Derivation of the Explicit Formula

Based on the kinetic model presented by Cai et al. (Cai et al., 2021), the formula of pseudo-steady-state cluster concentrations and nucleation rates is as follows:

$$[A_1B_1]=[\mathrm{SA_{tot}}]-[A], \tag{S1}$$

$$[A_1B_1]=\frac{\beta_{1\text{-}2}[A][B]}{\beta_{1\text{-}3}[A]+\beta_{3\text{-}3}[A_1B_1]+\beta_{3\text{-}5}[A_2B_2]+\beta_{3\text{-}6}[A_3B_3]+\beta_{3\text{-}7}[A_4B_4]+\mathrm{CoagS_3}+\gamma}, \tag{S2}$$

$$[A_2B_1]=\frac{\beta_{1\text{-}3}[A][A_1B_1]}{\beta_{2\text{-}4}[B]+\mathrm{CoagS_4}}, \tag{S3}$$

$$[A_2B_2]=\frac{\frac{1}{2}\beta_{3\text{-}3}[A_1B_1][A_1B_1]+\beta_{2\text{-}4}[A_2B_1][B]}{\beta_{3\text{-}5}[A_1B_1]+\beta_{5\text{-}5}[A_2B_2]+\mathrm{CoagS_5}}, \tag{S4}$$

$$[A_3B_3]=\frac{\beta_{3\text{-}5}[A_2B_2][A_1B_1]}{\beta_{3\text{-}6}[A_1B_1]+\mathrm{CoagS_6}}, \tag{S5}$$

$$[A_4B_4]=\frac{\beta_{3,\,6}[A_3B_3][A_1B_1]+\frac{1}{2}\beta_{5,\,5}[A_2B_2][A_2B_2]}{\beta_{3,\,7}[A_1B_1]+\mathrm{CoagS_7}}, \tag{S6}$$

$$J_{A_4B_4}=\beta_{3,\,6}[A_3B_3][A_1B_1]+\frac{1}{2}\beta_{5,\,5}[A_2B_2][A_2B_2], \tag{S7}$$

where $[\mathrm{SA_{tot}}]$ represents the concentrations of sulfuric acid (SA) molecules or clusters containing one SA molecule, $A$ is SA molecules, $B$ is dimethylamine (DMA) molecules, and $A_mB_n$ is the clusters consisting of m SA molecules and n DMA molecules. $\beta_{i\text{-}j}$ ($m^3\ s^{-1}$) represents the collision coefficients ($\beta$) between molecules or clusters $i$ and $j$, and 1-7 represent $A$, $B$, $A_1B_1$, $A_2B_1$, $A_2B_2$, $A_3B_3$, and $A_4B_4$, respectively. Similarly, $\mathrm{CoagS}_i$ represents the coagulation sinks of molecules or clusters $i$. $\gamma$ ($s^{-1}$) is the evaporation rate of $A_1B_1$ clusters. Here the concentrations of clusters are shown as $[A_mB_n]$ in $m^{-3}$.

The analytical solution should be simplified based on proper approximations. For typical polluted urban areas, the sink of $A_1B_1$ is mainly due to the coagulation scavenging and evaporation, that is,

$$[A_1B_1]\approx\frac{\beta_{1\text{-}2}[A][B]}{\mathrm{CoagS_3}+\gamma}, \tag{S8}$$

however, for a wider range of atmospheric environments with lower CS and temperatures, the above approximations might lead to an overestimation of SA-DMA nucleation rates. Thus in this study, the self-coagulation of $A_1B_1$ and coagulation with $A$ would also be taken into account as a sink of $A_1B_1$:

$$[A_1B_1]\approx\frac{\beta_{1\text{-}2}[A][B]}{\beta_{1\text{-}3}[A]+\beta_{3\text{-}3}[A_1B_1]+\mathrm{CoagS_3}+\gamma}\approx\frac{\beta_{1\text{-}2}[A][B]}{\beta_{1\text{-}3}[\mathrm{SA_{tot}}]+\mathrm{CoagS_3}+\gamma}, \tag{S9}$$

Putting the above assumption together with the pseudo-steady-state nucleation rates formula, the explicit formula could be simplified to the version in the main text (Eqs. 8-11).

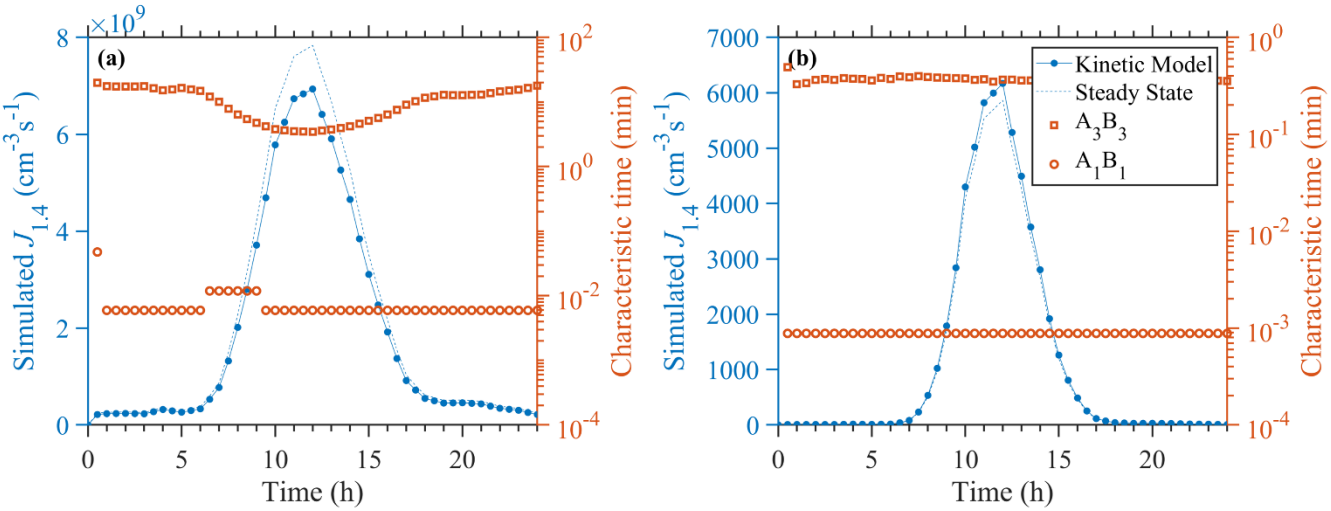


**Figure S1. Simulated $J_{1.4}$ (blue) and characteristic equilibrium time (red) of $A_3B_3$ and $A_1B_1$.** The typical conditions are [DMA]=3.0 pptv with $CS$=0.0001 $s^{-1}$ and $T$=255 K in (a) and $CS$=0.01 $s^{-1}$ and $T$=315 K in (b). The variation of SA concentrations is equal to the averaged diurnal variations.

## 3 Dimethylamine Emission inventory for marine area

Similar to the continental emission inventory for DMA, the maritime part is also built by combination of $NH_3$ emission inventory and DMA/$NH_3$ emission ratio. The maritime $NH_3$ emission is adopted from the results of Paulot et al with a grid transformation. The DMA/$NH_3$ emission ratio is estimated by the measured data from a previous study (Chen et al., 2021). During their maritime campaign, mean gaseous DMA and NH3 concentrations are 0.006 μg $cm^{-3}$ and 0.5300 μg $cm^{-3}$, of which 16% and 34% come from continental transport, respectively. Hence we can obtain the marine-originated DMA (0.0050 μg $cm^{-3}$) and $NH_3$ (0.34980 μg $cm^{-3}$) concentrations and an approximate DMA/$NH_3$ emission ratio of 0.0144.

**Table S2. Key parameters in simulating atmospheric sinks of dimethylamine**

| Sinks | This study | Variation range |
|---|---|---|
| Wet deposition (Henry Law's constant/mol $m^{-3}$ $Pa^{-1}$) | 0.56 | 0.3-0.6 (Sander, 2015) |
| Gas-phase reaction (•OH oxidation rate constant/$cm^{-3}$ $s^{-1}$) | $6.49 \times 10^{-11}$ | $(5.85\text{-}7.13) \times 10^{-11}$ (Carl and Crowley, 1998) |
| Aerosol uptake (Uptake coefficient) | 0.001 | $5.9 \times 10^{-4}$-$4.4 \times 10^{-2}$ (Qiu et al., 2011; Wang et al., 2010) |

## 4 Dependence of NPF occurrence in 3-D simulation results on CS

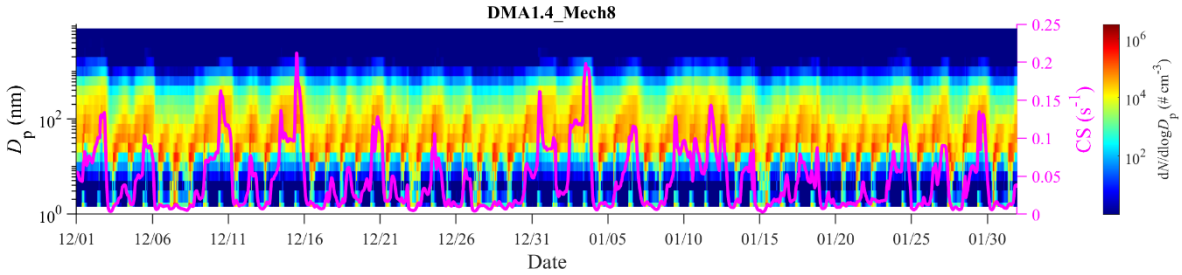


**Figure S2. Simulated Evolution of PNSDs and Timeseries of CS (violet line) from scenario DMA1.4_Mech8.**

## 5 Comparisons of simulations between DMA1.4_Mech8 and the scenario with a previous parameterization

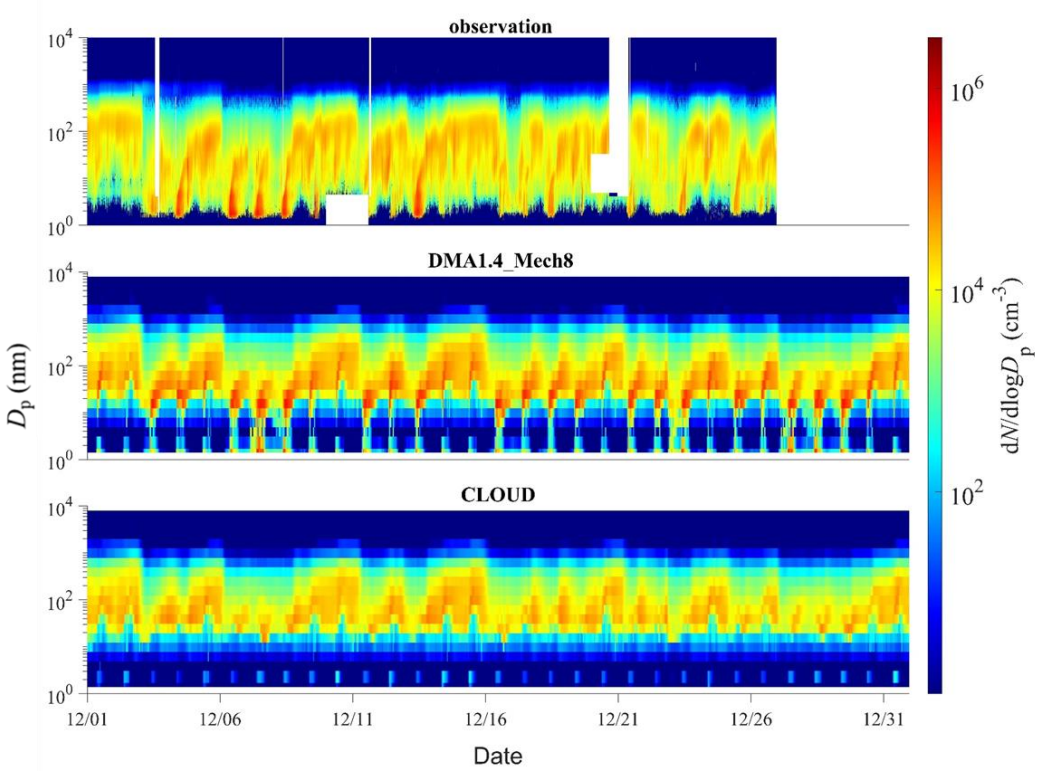


**Figure S3. Comparison of observed and simulated averaged particle number size distribution from scenarios with parameterizations from Dunne et al., 2016 (CLOUD) the original scenario (DMA1.4_Mech8).**

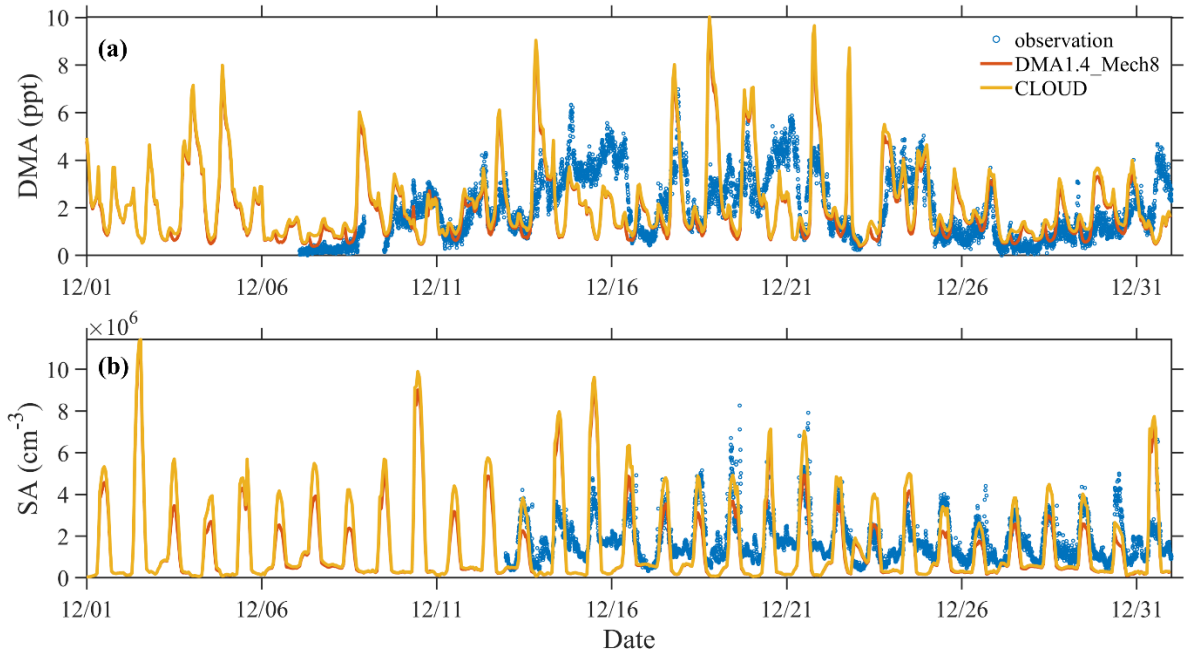


**Figure S4. Comparison of observed and simulated DMA (a) and SA (b) concentrations from scenarios with parameterizations from Dunne et al., 2016 (CLOUD) the original scenario (DMA1.4_Mech8).**

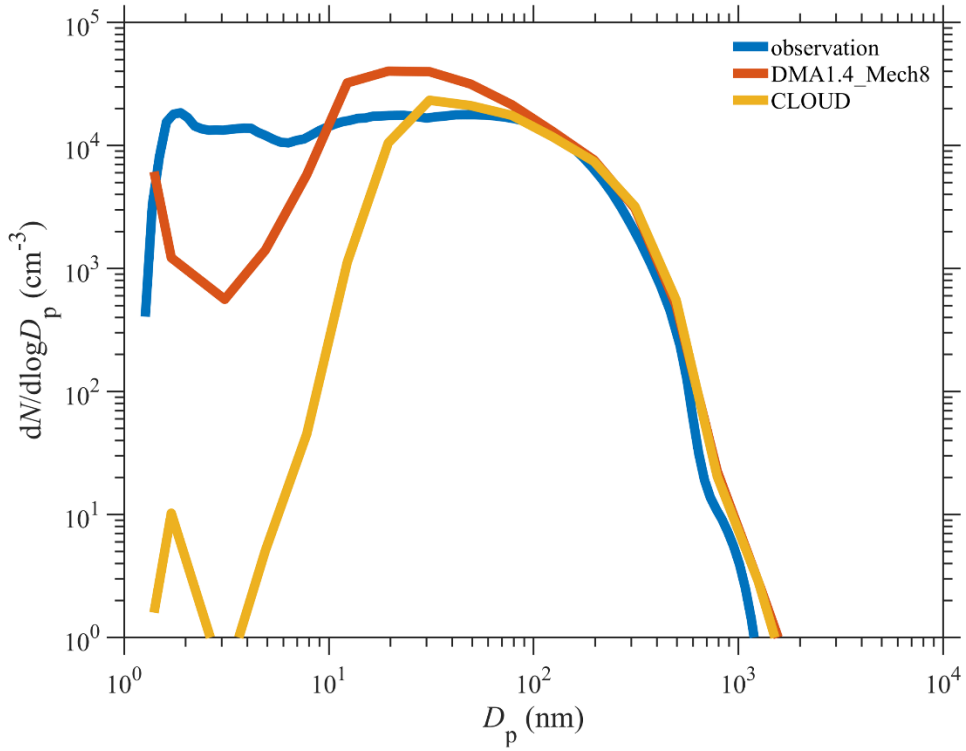


**Figure S5. Comparison of observed and simulated averaged particle number size distribution from scenarios with parameterizations from Dunne et al., 2016 (CLOUD) the original scenario (DMA1.4_Mech8).**

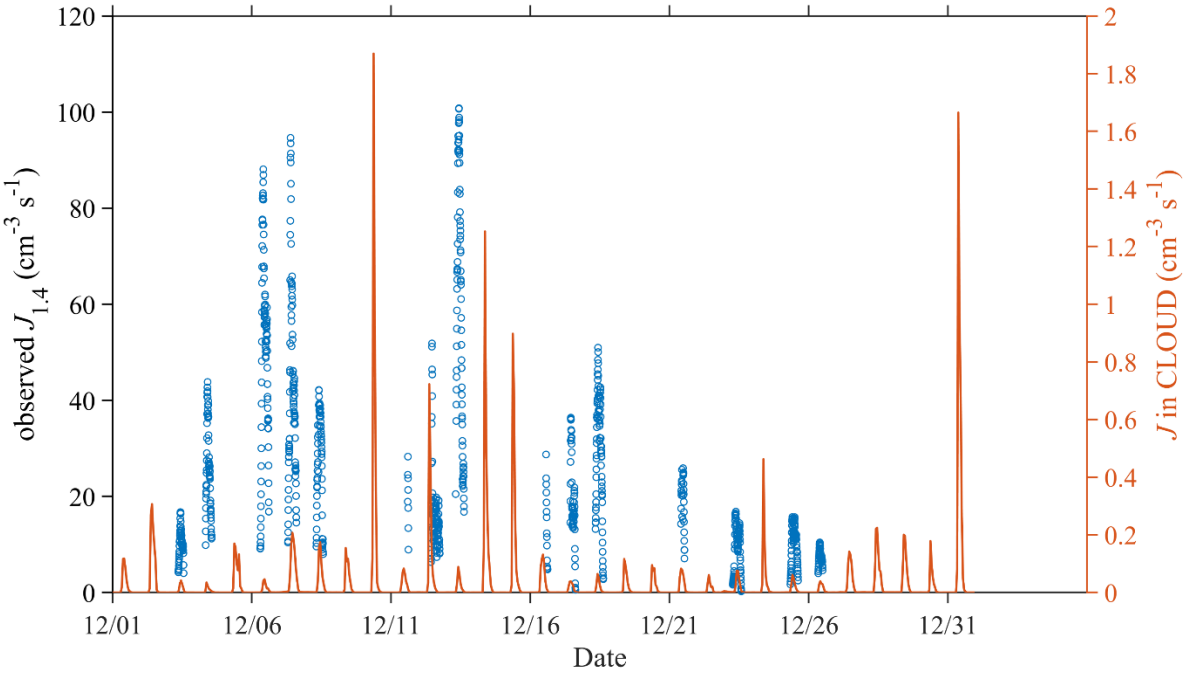


**Figure S6. Comparison of observed $J_{1.4}$ and simulated nucleation rates from scenarios with parameterizations from Dunne et al., 2016 (CLOUD).**

## 6 Sensitivity tests

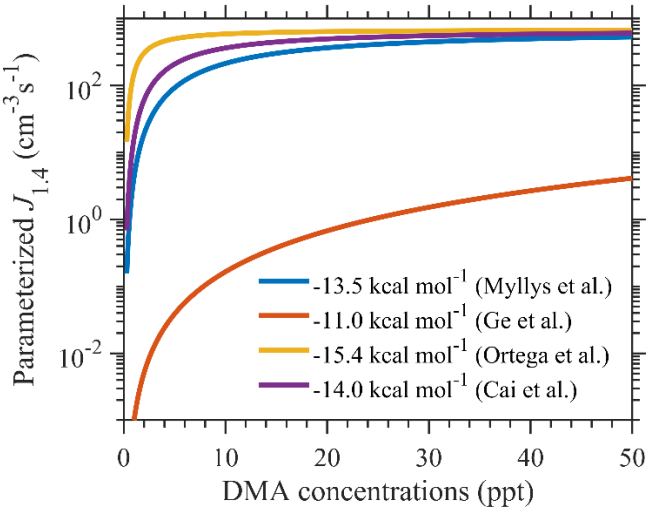


**Figure S7. Variation of parameterized J1.4 with DMA concentrations at 281 K with different ΔG values applied of -15.40, -14.00, -13.54, and -11.02 kcal mol-1, respectively.**

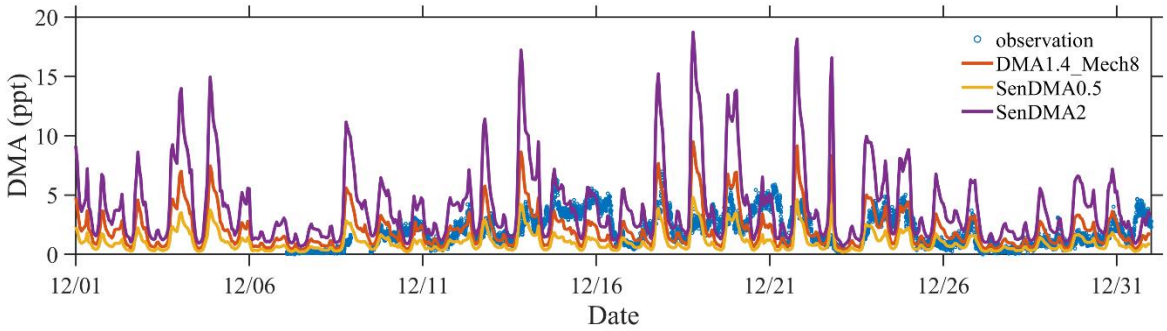


**Figure S8. Comparison of observed and simulated DMA concentrations from sensitivity scenarios of halving (SenDMA0.5) and doubling (SenDMA2) the DMA emission and the original scenario (DMA1.4_Mech8).**

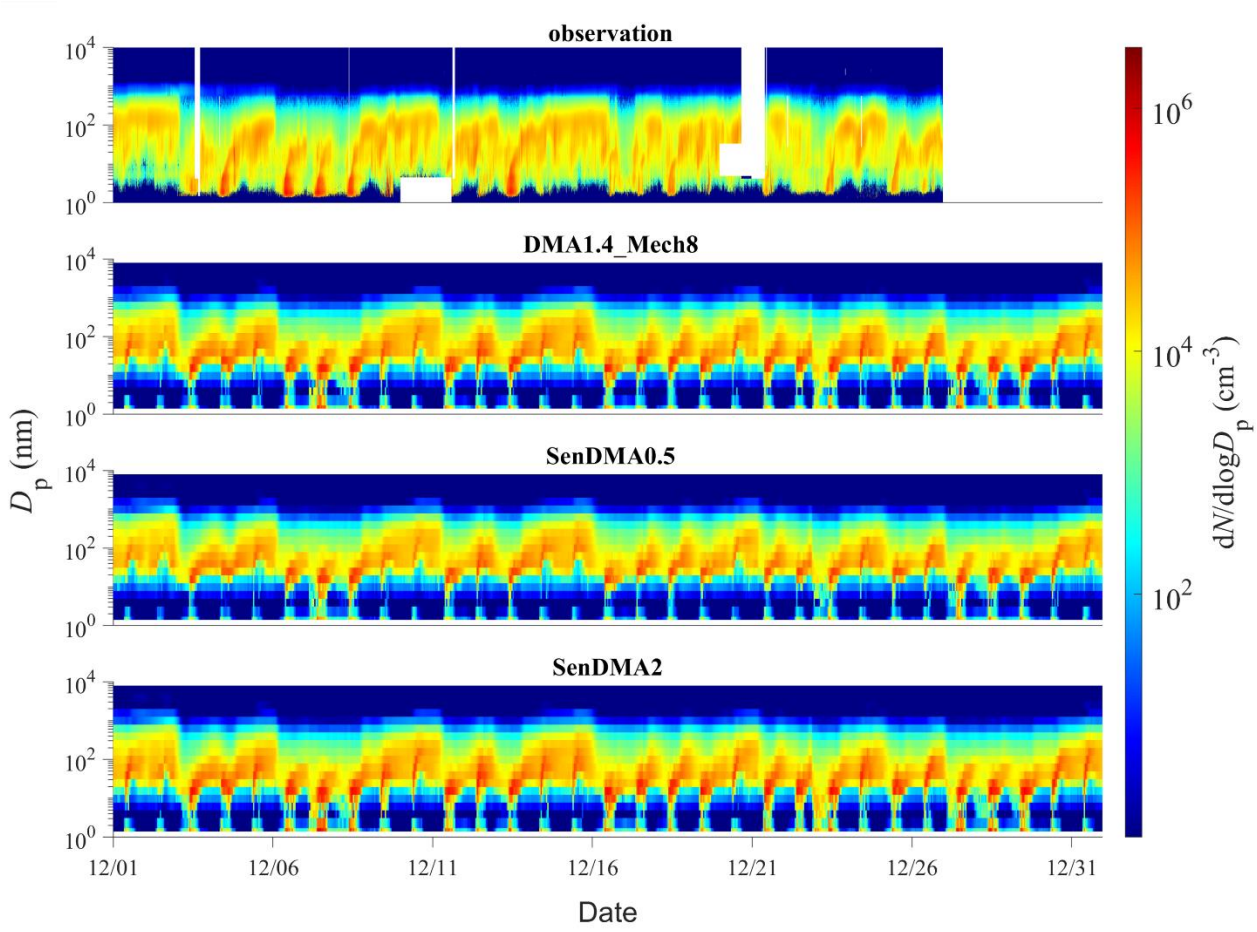


**Figure S9. Comparison of observed and simulated particle number size distribution from sensitivity scenarios of halving (SenDMA0.5) and doubling (SenDMA2) the DMA emission and the original scenario (DMA1.4_Mech8).**

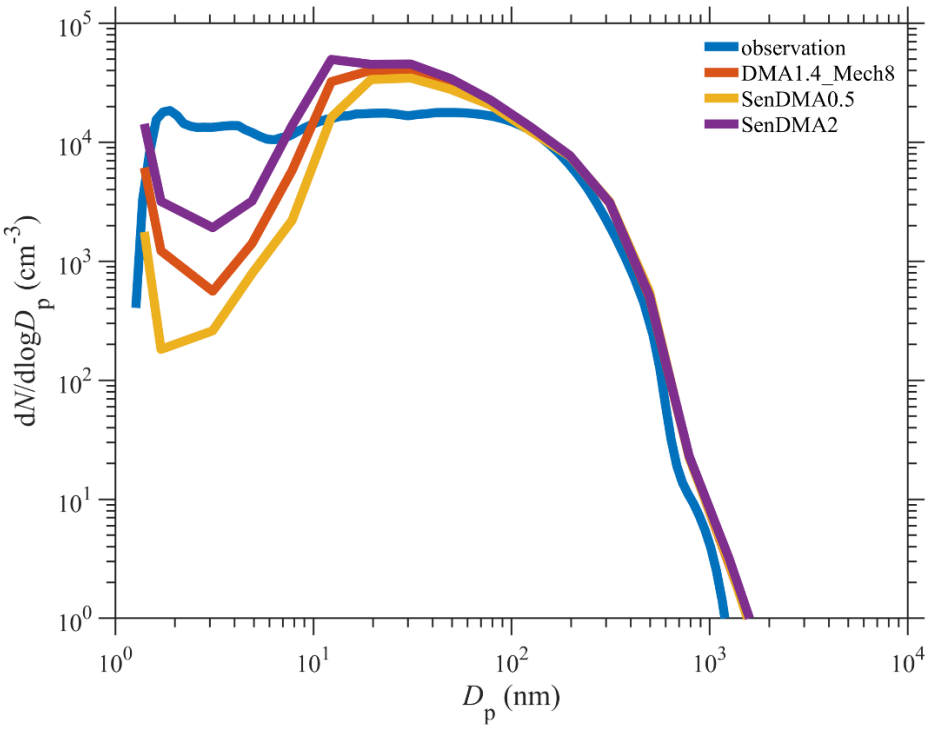


**Figure S10. Comparison of observed and simulated averaged particle number size distribution from sensitivity scenarios of halving (SenDMA0.5) and doubling (SenDMA2) the DMA emission and the original scenario (DMA1.4_Mech8).**

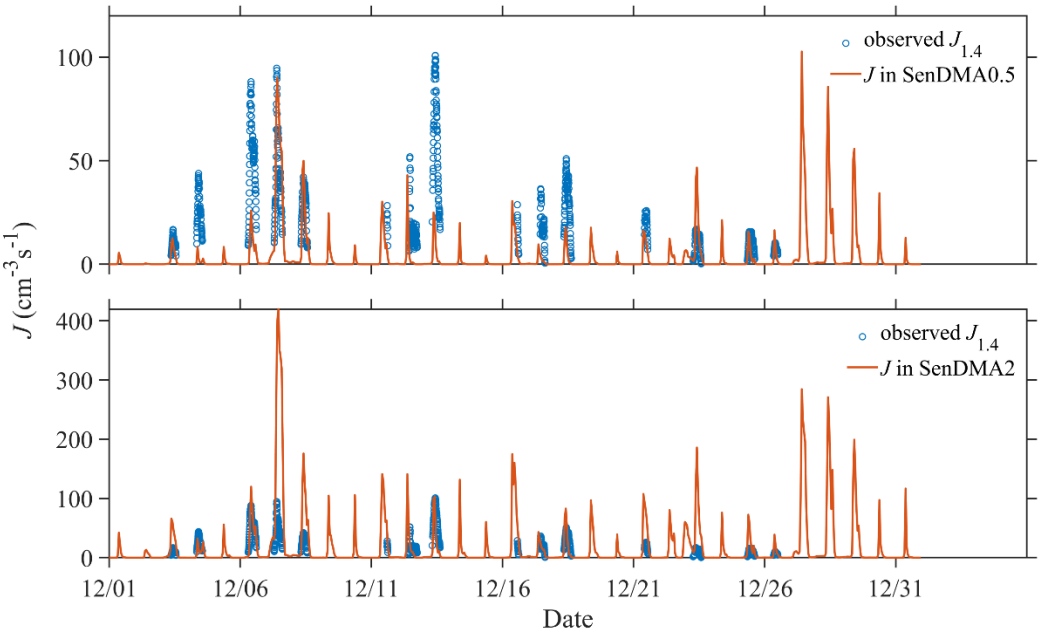


**Figure S11. Comparison of observed $J_{1.4}$ and simulated nucleation rate from sensitivity scenarios of halving (SenDMA0.5) (a) and doubling (SenDMA2) (b) the DMA emission.**

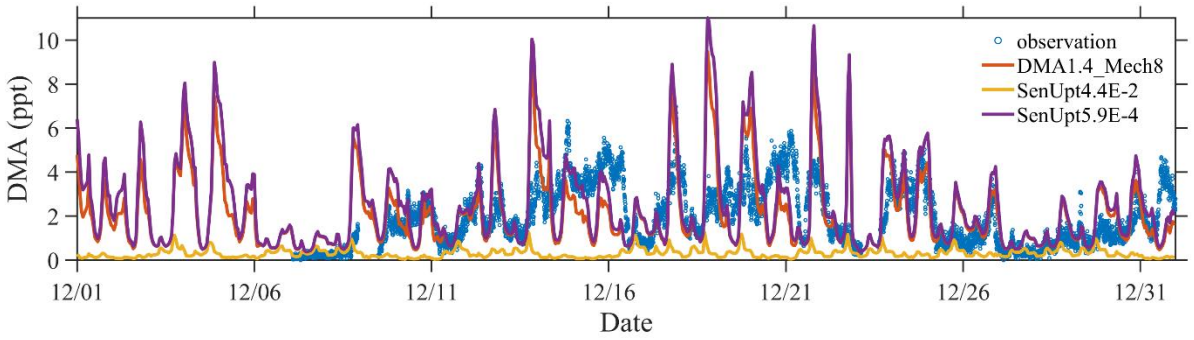


**Figure S12. Comparison of observed and simulated DMA concentrations from sensitivity scenarios using lowest (SenUpt5.9E-4) and highest (SenUpt4.4E-2) aerosol uptake coefficient of DMA and the original scenario (DMA1.4_Mech8).**

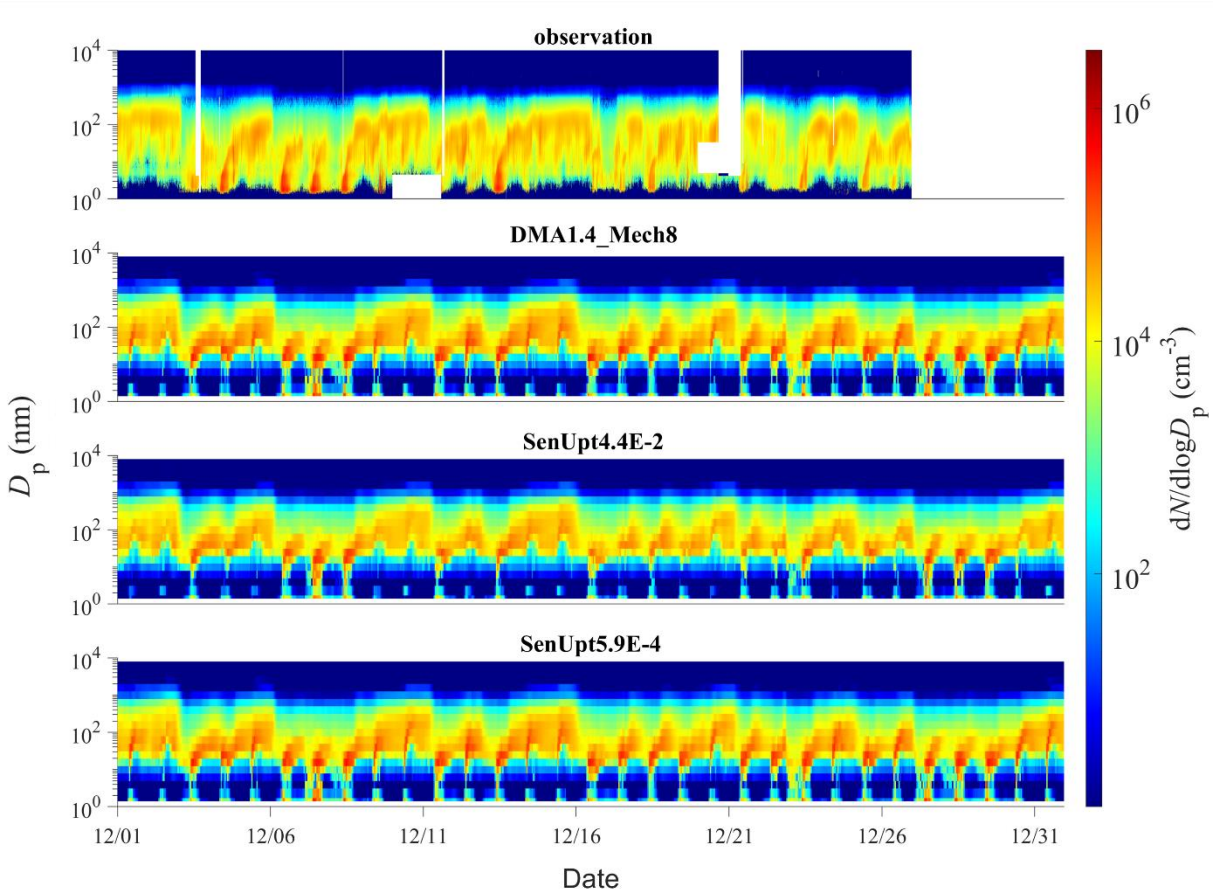


**Figure S13. Comparison of observed and simulated particle number size distribution from sensitivity scenarios using lowest (SenUpt5.9E-4) and highest (SenUpt4.4E-2) aerosol uptake coefficient of DMA and the original scenario (DMA1.4_Mech8).**

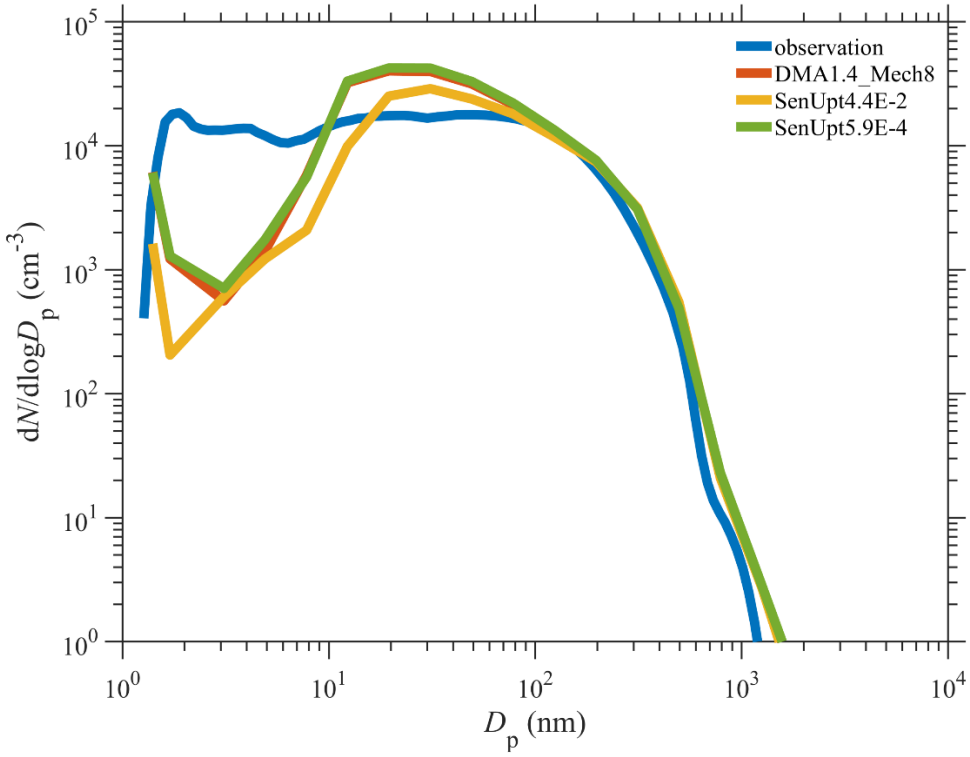


**Figure S14. Comparison of observed and simulated averaged particle number size distribution from sensitivity scenarios using lowest (SenUpt5.9E-4) and highest (SenUpt4.4E-2) aerosol uptake coefficient of DMA and the original scenario (DMA1.4_Mech8).**

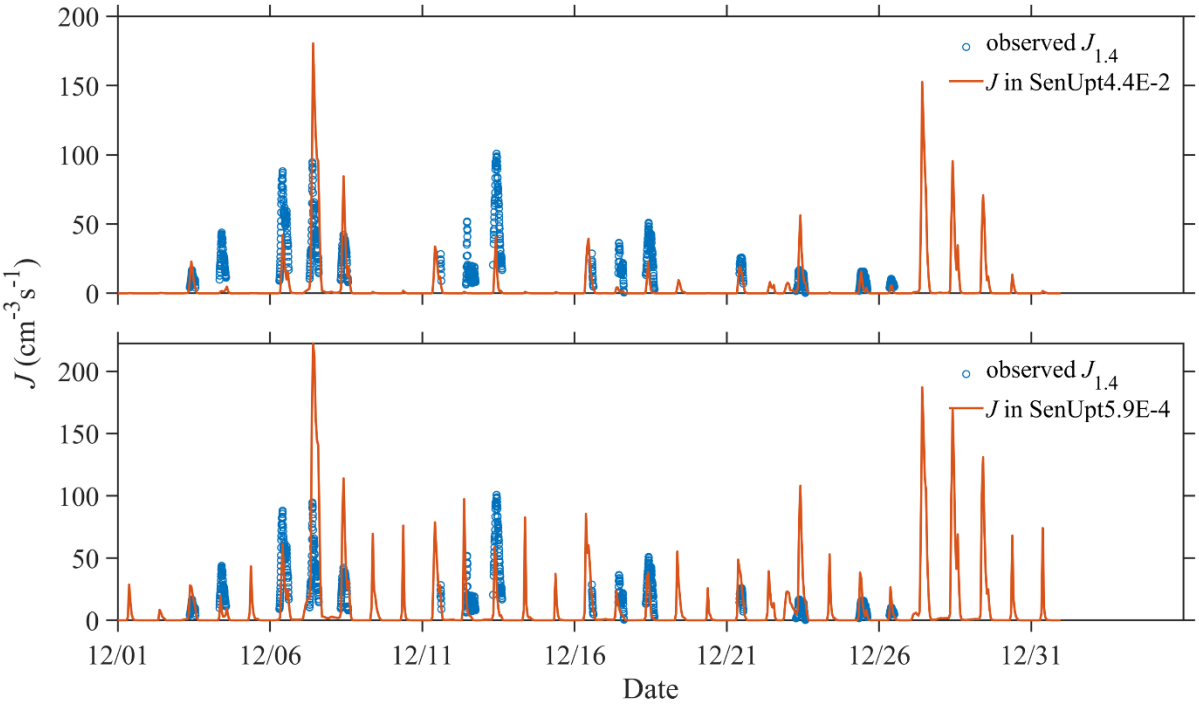


**Figure S15. Comparison of observed $J_{1.4}$ and simulated nucleation rate from sensitivity scenarios using lowest (SenUpt5.9E-4) (a) and highest (SenUpt4.4E-2) (b) aerosol uptake coefficient of DMA and the original scenario (DMA1.4_Mech8).**

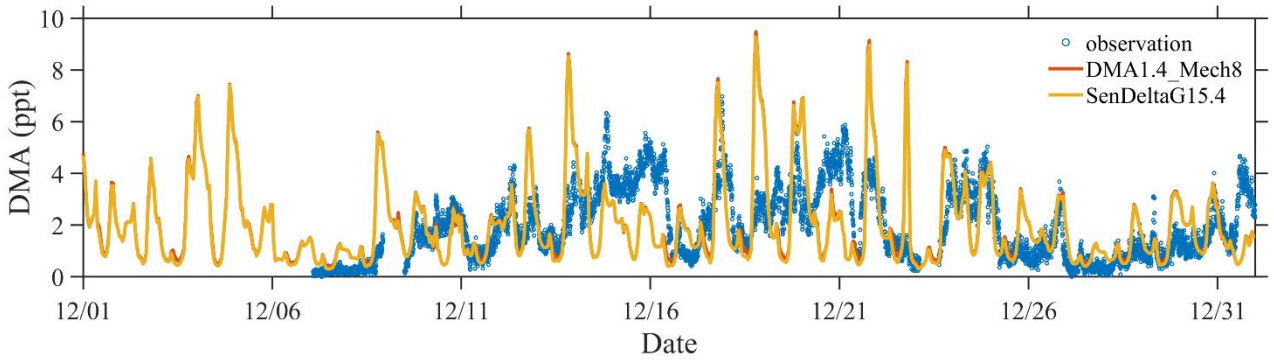


**Figure S16. Comparison of observed and simulated DMA concentrations from sensitivity scenarios using ΔG = -15.4 kcal mol$^{-1}$ (SenDeltaG15.4) and the original scenario (DMA1.4_Mech8).**

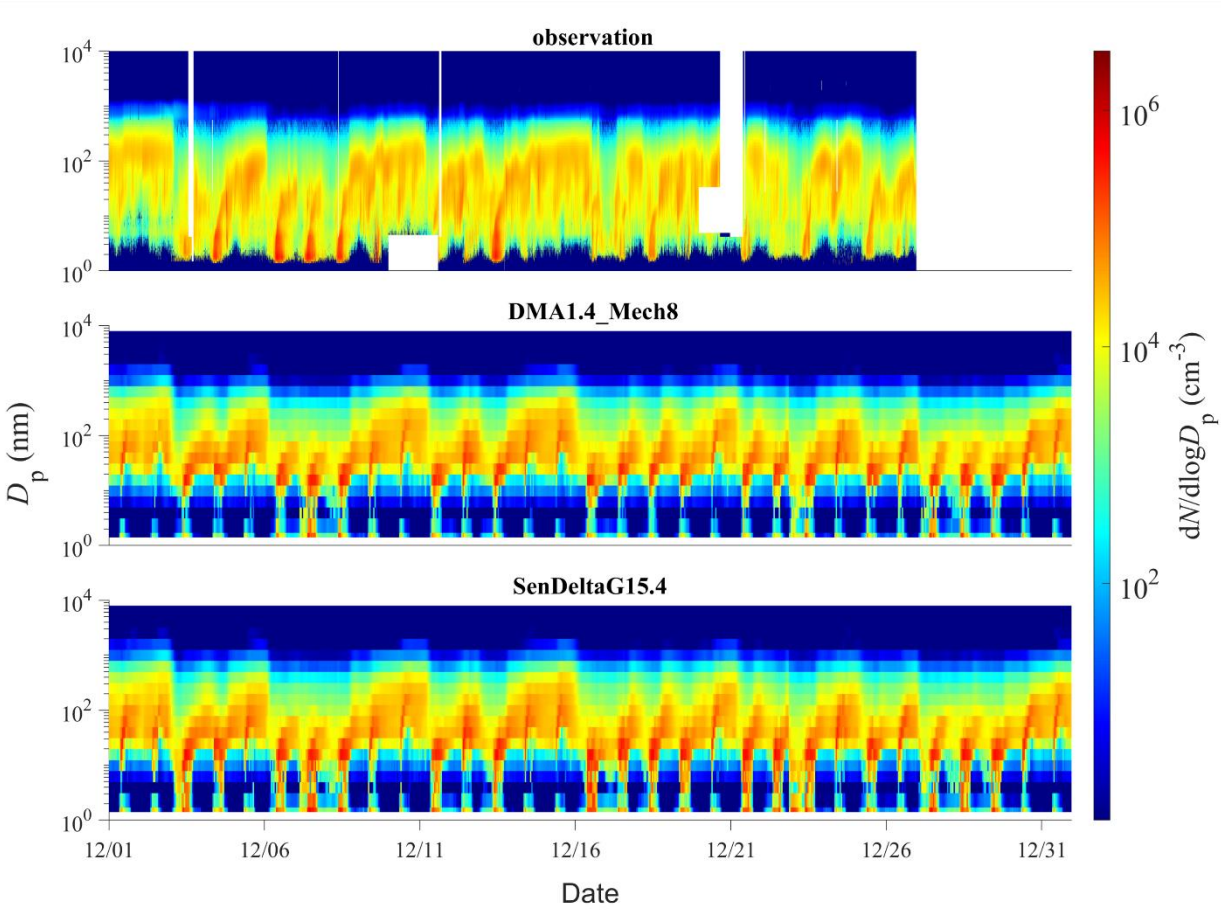


**Figure S17. Comparison of observed and simulated particle number size distribution from sensitivity scenario using ΔG = -15.4 kcal mol$^{-1}$ (SenDeltaG15.4) and the original scenario (DMA1.4_Mech8).**

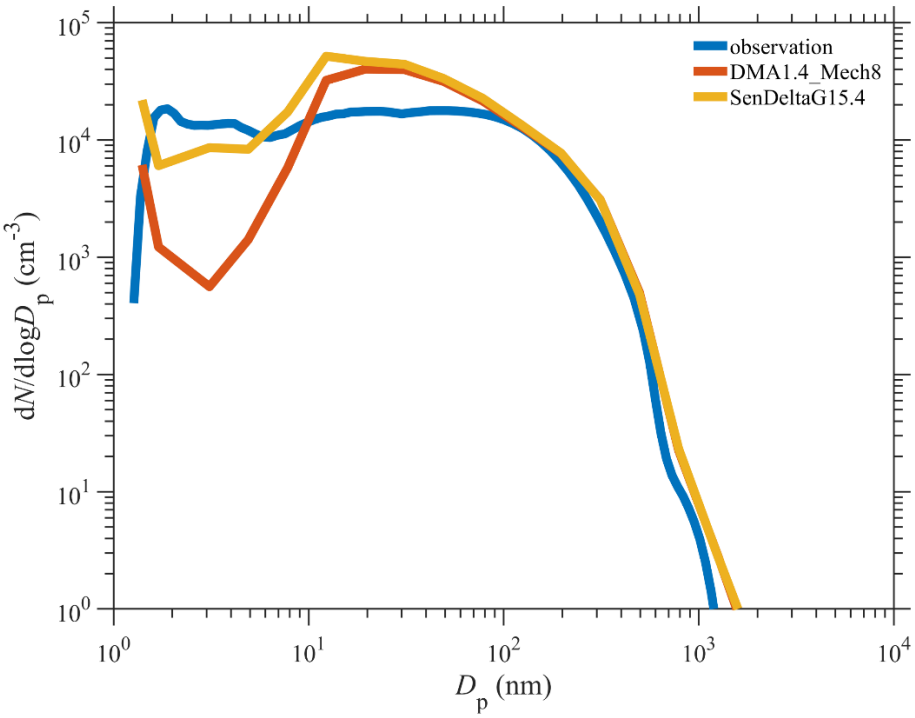


**Figure S18. Comparison of observed and simulated averaged particle number size distribution from sensitivity scenarios using ΔG = -15.4 kcal mol$^{-1}$ (SenDeltaG15.4) and the original scenario (DMA1.4_Mech8).**

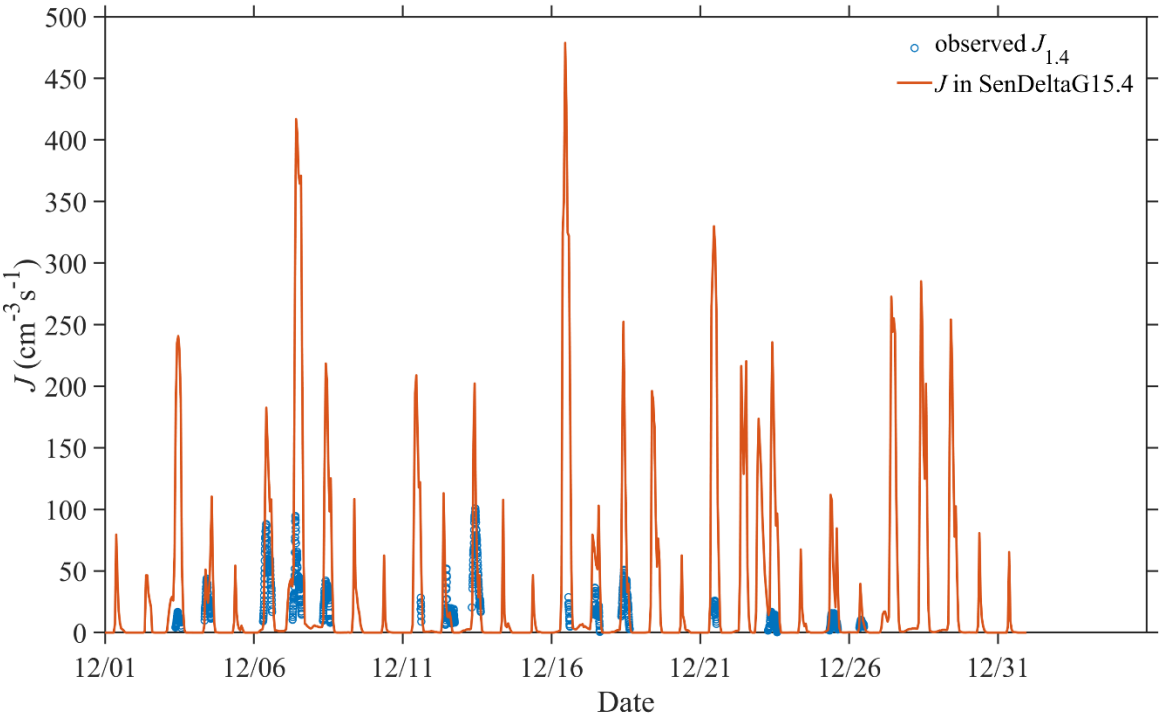


**Figure S19. Comparison of observed $J_{1.4}$ and simulated nucleation rates from sensitivity scenarios using ΔG = -15.4 kcal mol$^{-1}$ (SenDeltaG15.4).**

**References:**


Cai, R. L., Yan, C., Yang, D. S., Yin, R. J., Lu, Y. Q., Deng, C. J., Fu, Y. Y., Ruan, J. X., Li, X. X., Kontkanen, J., Zhang, Q., Kangasluoma, J., Ma, Y., Hao, J. M., Worsnop, D. R., Bianchi, F., Paasonen, P., Kerminen, V. M., Liu, Y. C., Wang, L., Zheng, J., Kulmala, M., and Jiang, J. K.: Sulfuric acid-amine nucleation in urban Beijing, Atmos Chem Phys, 21, 2457-2468, 2021.

Carl, S. A. and Crowley, J. N.: Sequential Two (Blue) Photon Absorption by $NO_2$ in the Presence of $H_2$ as a Source of OH in Pulsed Photolysis Kinetic Studies: Rate Constants for Reaction of OH with $CH_3NH_2$, $(CH_3)_2NH$, $(CH_3)_3N$, and $C_2H_5NH_2$ at 295 K, The Journal of Physical Chemistry A, 102, 8131-8141, 10.1021/jp9821937, 1998.

Chen, D., Shen, Y., Wang, J., Gao, Y., Gao, H., and Yao, X.: Mapping gaseous dimethylamine, trimethylamine, ammonia, and their particulate counterparts in marine atmospheres of China's marginal seas – Part 1: Differentiating marine emission from continental transport, Atmos Chem Phys, 21, 16413-16425, 10.5194/acp-21-16413-2021, 2021.

Qiu, C., Wang, L., Lal, V., Khalizov, A. F., and Zhang, R.: Heterogeneous reactions of alkylamines with ammonium sulfate and ammonium bisulfate, Environ Sci Technol, 45, 4748-4755, 10.1021/es1043112, 2011.

Sander, R.: Compilation of Henry's law constants (version 4.0) for water as solvent, Atmos Chem Phys, 15, 4399-4981, 10.5194/acp-15-4399-2015, 2015.

Wang, L., Lal, V., Khalizov, A. F., and Zhang, R.: Heterogeneous Chemistry of Alkylamines with Sulfuric Acid: Implications for Atmospheric Formation of Alkylaminium Sulfates, Environmental Science & Technology, 44, 2461-2465, 10.1021/es9036868, 2010.